The Very Large Hadron Collider Beam Collimation System *

A.I. Drozhdin, N.V. Mokhov, A.A. Sery, Fermilab, P.O. Box 500, Batavia, IL 60510 USA

1 INTRODUCTIONS

Even in good operational conditions, a finite fraction of the beam will leave the stable central area of accelerator because of beam-gas interactions everywhere along the accelerator, intra-beam scattering, collisions in the IPs, RF noise, ground motion and resonances excited by the accelerator imperfections producing a beam halo. As a result of beam halo interactions with limiting aperture, hadronic and electromagnetic showers are induced in accelerator and detector components causing accelerator related background in the detectors, magnets heating and accelerator and environment irradiation. A beam collimation system is used for the beam halo interception in a specially equipped warm part of accelerator.

A multi-turn particle tracking through the accelerator and beam halo interactions with the collimators are done with STRUCT [1] code. All lattice components with their strength and aperture restrictions are taken into account during these calculations. Particles lost in the accelerator are stored in the files for the next step of calculations using MARS [2]code.

(((Full scale Monte-Carlo hadronic and electromagnetic shower simulations, secondary particles transport in the accelerator and detector components, including shielding with real materials and magnetic fields are done with MARS.)))

2 RESULTS OF SIMULATIONS

A main purpose of the VLHC beam cleaning system is to reduce accelerator related backgrounds in the detector and to decrease beam loss rates in superconducting magnets.

We assumed that the beam intensity at the beginning of collisions is $2{\cdot}10^{14}\,ppp$ [3], and the run duration is 10 hours. If intensity drops during the run by 10% because of elastic interactions in the IP, ground motion and resonances, this amounts the rate of particle loss in the collimation system of $6 \cdot 10^{8}\ p/s$. The total power of beam loss is $4.5\ kW$. A r.m.s. normalized emittance of the beam is assumed to be $1.3\ mm \cdot mrad$ [3]. We assumed also beam pipe aperture in the utility section of R=20 mm, and in the low-β IP and accelerator arc of R=18 mm.

A two-stage [4] beam collimation system is designed for the VLHC to localize most of losses in the utility straight section [5] specially designed to match the requirements of beam collimation and abort systems. Maximum of dispersion in the accelerator arc is equal to $3.32m$, and zero in the interaction region (IR). β-functions in the VLHC low-β IR and arc lattice are shown in Figures 1 and 2 for collision optics. The collimation system consists of horizontal and vertical primary collimators and a set of secondary collimators placed at an optimal phase advance, to intercept most of particles outscattered from the primary collimators during the first turn after particle interaction with primary collimator. Particle impact parameter on a primary collimator is of the order of 1μm [6]. A thin primary collimator increases proton amplitude as a result of multiple Coulomb scattering and thus effects in drastic increase of particle impact parameter on the downstream secondary collimators. This results in a significant reduction of the outscattered proton yield and total beam loss in the accelerator, decreases collimator jaws overheating and mitigates requirements to collimators alignment.

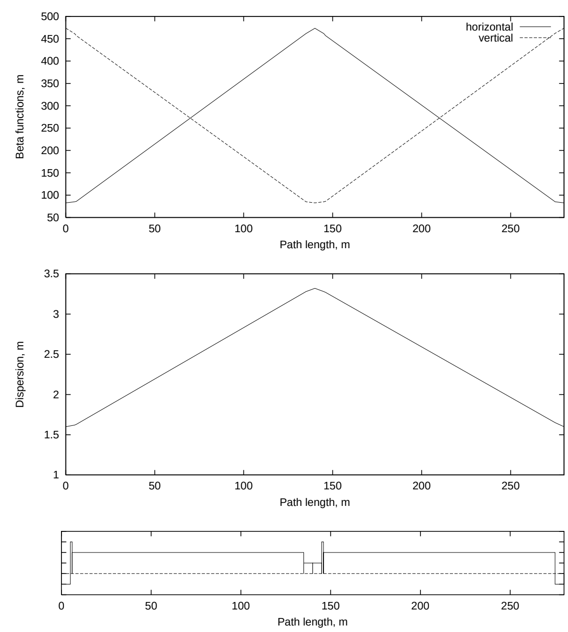

Figure 1: Beta functions and dispersion in the VLHC arc.

Collimation system location in the utility section is shown in Figure 3. KM, LAMB and SM are kicker, Lambertson and septum magnets of the beam abort system not described here. A primary horizontal collimator PriHp located in the beginning of utility section in the large dispersion region is used for positive sign off-momentum particles collimation. Particles scattered by the primary collimator are intercepted by the secondary collimators SHp030 and SHp330 located in 17^{o} and 350^{o} phase advance downstream of the primary collimator.

Proton transverse populations in the primary collimator and secondary collimators are shown in Figure 4. In our

* Work supported by the U. S. Department of Energy under contract No. DE-AC02-76CH03000

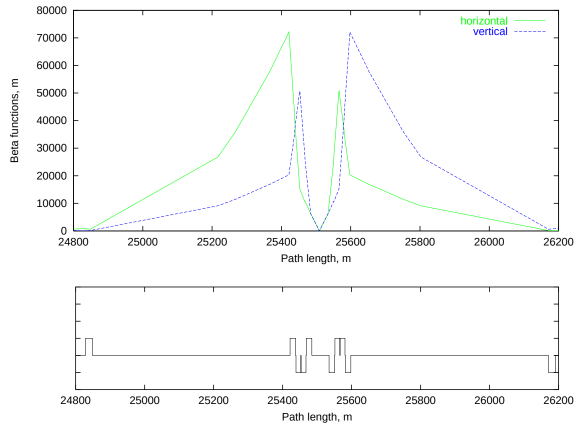

Figure 2: Beta functions in the IR.

simulations particles first time interact primary collimator with a small (about $3\mu m$) impact parameter. As a result of multiple Coulomb scattering in the primary collimator, the impact parameter at the secondary collimators, increases to about $0.1mm$ (Figure 5).

A primary horizontal collimator PriHm located in the center of utility section in the high dispersion region is used for negative sign off-momentum protons collimation. Collimators SHm030 located in 8^o, and SHp330 located in 165^o behind the primary collimator are used as a secondary collimators. Unfortunately secondary collimator SHp330 must be located from both sides of the beam to intercept both positive and negative signs off-momentum particles. This is the only place with aperture restrictions from both sides of the circulating beam. Proton transverse populations in these collimators are shown in Figure 6. Primary momentum collimators PriHp and PriHm placed at $10\sigma_x$ intercept protons with momentum deviations bigger than $\pm 3 \cdot 10^{-4}$.

A primary horizontal collimator PriH located in the large β-function and zero dispersion region is used for large amplitude particles collimation. Collimators SH030 located in 9^o, and SH150 located in 170^o behind the primary collimator are used as a secondary collimators. Proton transverse populations in these collimators are shown in Figure 7.

Vertical primary collimator PriV and secondary collimators SV030 (phase 8^o) and SV150 (phase 137^o) are used for halo collimation in the vertical plane (Figure 8).

After the first interaction with primary collimator high amplitude particles are intercepted by the secondary collimators, but large number of particles survive, and will interact with primary collimator again. Average number of particle interactions is equal to 1.4 if primary collimators are placed at 10 σ and secondary at 12 σ. Particles with amplitudes smaller than 12σ are not intercepted by the secondary collimators, and survive during several tens turns until they increase amplitude at the next interactions with primary collimator. These particles occupy region inside the 12σ envelope.

Although primary collimators are placed at 10σ and secondary collimators are at 12σ from the beam axis, the tail of halo is extended behind 12σ. Halo particles population and amplitude distribution in the accelerator aperture are shown in Figure 9 for collimation of equilibrium particles, and in Figure 10 for off-momentum particles with $dP/P = \pm 10^{-4}$. Large amplitude particles, which escape from the cleaning system at the first turn, are able to circulate in the machine, before being captured by the collimators on the later turns. This defines the machine geometric aperture.

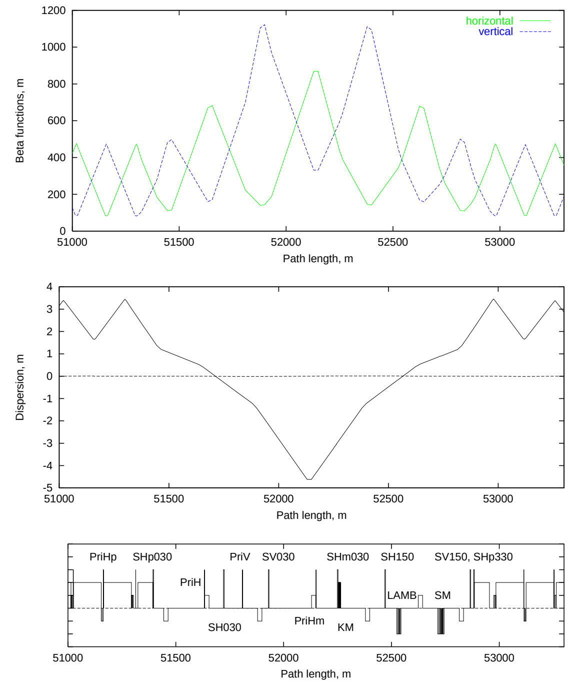

Figure 3: Beta functions and dispersion in the collimation system location.

Beam loss distribution in the VLHC with primary collimators at 10σ and secondary collimators at 12σ is presented in Figures 11 (top). We assumed that 25% of halo interact first with each of four primary collimators.

As is seen from Figures 4 - 10, particles amplitude growth at interaction with $10mm$ tungsten primary collimator is pretty large compared to the beam size and is comparable to the accelerator aperture (13σ), that causes particle loss in the IR quads. Our studies show that in the VLHC, a $5mm$ thick tungsten primary collimator positioned at 5σ from the beam axis in vertical or horizontal planes would function as an optimal primary collimator. At 50 TeV, an optimal length of copper secondary collimator equals 3 m. Collimators jaw is positioned at 6.2σ from the beam center in horizontal or vertical plane. To decrease outscattered particles flux from the secondary collimators they are aligned parallel to the circulating beam envelope.

The beam collimation utility section is designed using normalconducting magnets. The beam loss in the utility section amounts $240\ W/m$, which is not a big problem for normalconducting elements. The maximum beam loss in the superconducting part of accelerator occurs in

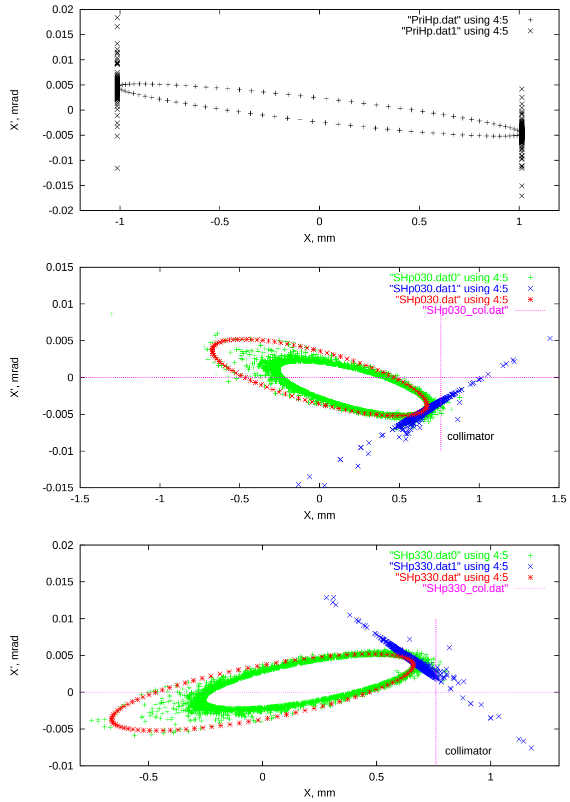

Figure 4: Horizontal halo population at the primary PriHp collimator exit (top), in the secondary collimator SHp030 (middle), and in the secondary collimator SHp330 (bottom). Ellipse represents 10σ envelope on the phase plane. Black crosses represent particles at the first turn after interaction with the primary collimator (without secondary collimators).

the 16 m long quadrupoles in the IP. The main reason is that the β function reaches its maximum in the final focus quadrupoles. This maximum is equal to $3.24\ W/m$ or $4.06 \cdot 10^5 p/(m \cdot sec)$ for primary collimators at 10σ and secondary collimators at 12σ, and $1.24\ W/m$ or $1.55 \cdot 10^5 p/(m \cdot sec)$ for primary collimators at 5σ and secondary collimators at 6.2σ. As a reference we can consider the LHC admissible limits for superconducting magnets, which is equal to $7 \cdot 10^6 p/(m \cdot sec)$ [8] for $7TeV$ and scale it by a ratio of accelerators energy (50/7=7). The VLHC collimation system permits to decrease losses in the superconducting magnets to a level which is two times below the admissible limit even if collimators are at 10σ and 12σ.

Two more supplementary collimators are placed in the IR in the distance of $270m$ upstream and downstream of quadrupoles to decrease particle losses in the low-β quadrupoles. They are located at $10\sigma_{x,y}$ to intercept only particles outscattered from the secondary collimators. Phase advance between the supplementary collimator and low-β quadrupoles is small, that permits to keep quadrupoles in a shadow of supplementary collimators. This eliminates primary particle flux in the IP quads with

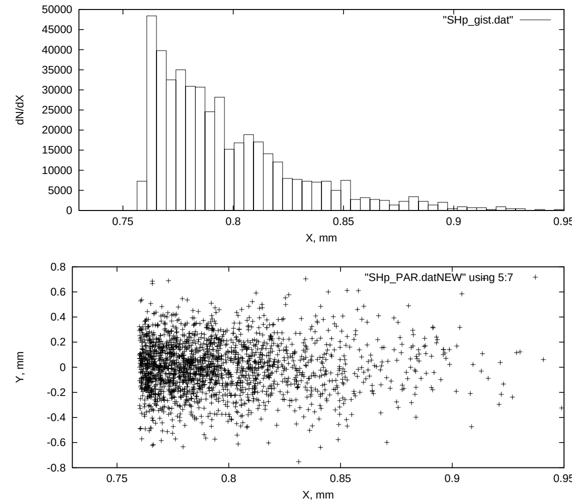

Figure 5: Proton transverse population in the secondary collimator SHp030.

primary collimators at 5σ, secondary collimators at 6.2σ and supplementary collimators at 10σ, and decreases flux by two order of magnitude to a level of $0.033\ W/m$ or $4.12 \cdot 10^3 p/(m \cdot sec)$ with primary collimators at 10σ and supplementary collimators at 13σ. Beam loss distribution in the VLHC with primary collimators at 5σ, secondary collimators at 6.2σ and supplementary collimators at 10σ is presented in Figures 11 (bottom).

The most irradiated superconducting magnet with supplementary collimators is one of the first 129 m long magnets and 5 m long quadrupole behind the collimation system. Beam loss rate in this magnet is equal to $0.022\ W/m$ ($2.75 \cdot 10^3 p/(m \cdot sec)$), in the quadrupole - $0.089\ W/m$ ($1.11 \cdot 10^4 p/(m \cdot sec)$) with primary collimators at 5σ, what is two order of magnitude below the admissible limit.

A beam loss analysis has shown that the accelerator related background in the detector is originated by particle loss in the inner triplet region. There are two possible points of particle loss in this region - supplementary collimator and low-β quadrupoles if supplementary collimator is not used. Particle loss rate in the supplementary collimator is two times higher compared to loss in the quadrupoles (See Figures 13), but collimator is located in sufficiently larger distance from the detector (358 m from the IP). Beam loss rate from one beam in the supplementary collimator is equal to $1.36 \cdot 10^7 p/sec$. Rate in the low-β quadrupoles without supplementary collimator from one side of IP is equal to $5.63 \cdot 10^6 p/sec$ (incoming beam) and $3.43 \cdot 10^6 p/sec$ from other side (outgoing beam) for primary collimators at 5σ.

3 CONCLUSIONS

The utility straight section is designed to match the requirements of beam collimation and abort systems. A two-stage beam collimation system consists of $5mm$ thick primary tungsten collimators placed at $5\sigma_{x,y}$, and $3m$ long

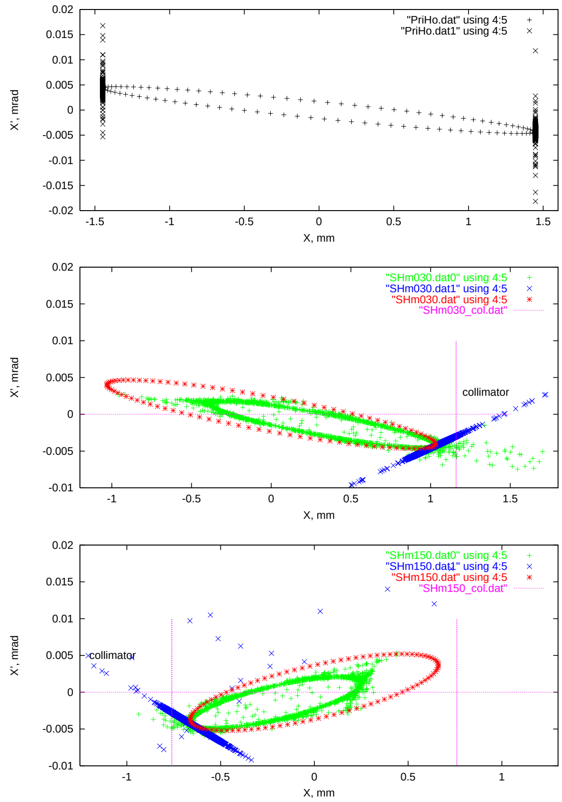

Figure 6: Horizontal halo population at the primary PriHm collimator exit (top), in the secondary collimator SHm030 (middle), and in the secondary collimator SHp330 (bottom).

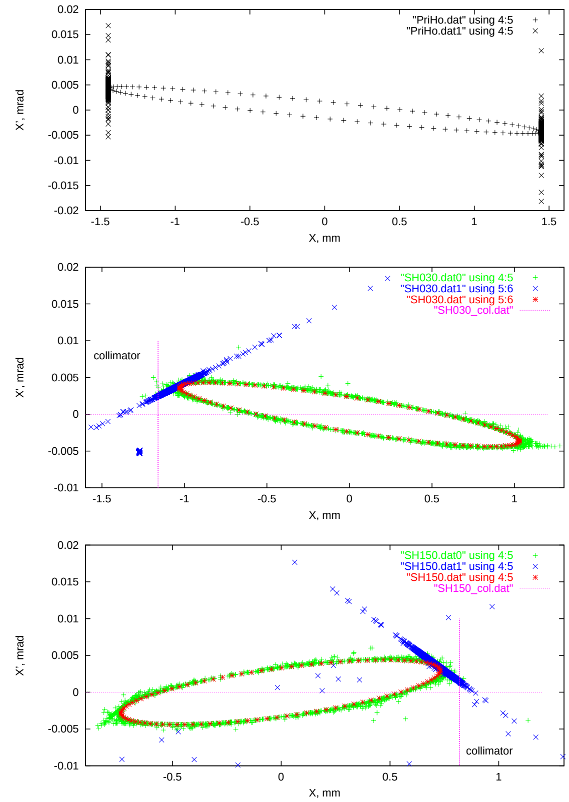

Figure 7: Horizontal halo population at the primary PriH collimator exit (top), in the secondary collimator SH030 (middle), and in the secondary collimator SH150 (bottom).

copper secondary collimators located in an optimal phase advance at $6.2\sigma_{x,y}$ and aligned parallel to the circulating beam envelope. Two more supplementary collimators are placed in the IR in a distance of $270m$ upstream and downstream of quadrupoles to decrease particle losses in the low-β quadrupoles. They are located at $10\sigma_{x,y}$ to intercept only particles outscattered from the secondary collimators.

The effect of beam cleaning system operation on the particle loss distribution in the entire machine is calculated with emphasis on high luminosity insertions and the detector backgrounds.

The maximum beam loss in the superconducting part of accelerator occurs in the first magnets behind the collimation system. The maximum beam loss rate in this magnet is equal to $0.089\ W/m$ or $1.11 \cdot 10^4 p/(m \cdot sec)$ with primary collimators at 5σ, what is two order of magnitude below the admissible limit. The low-β quadrupoles heating from the beam cleaning adds smaller than 1% to the total heat load determined mostly by the pp collisions in the IP.

Beam loss rate from one beam in the supplementary collimator located in 358 m from the IP is equal to $1.36 \cdot 10^7 p/sec$, and there is no primary particle loss in the low-β quadrupoles with supplementary collimators in the IR at $10\sigma_{x,y}$.

4 REFERENCES

[1] I. Baishev, A. Drozhdin, and N. Mokhov, ‘STRUCT Program User’s Reference Manual’, SSCL–MAN–0034 (1994).

[2] N. V. Mokhov, ‘The MARS Code System User’s Guide, Version 13(95)’, Fermilab–FN–628 (1995).

[3] “Very Large Hadron Collider”, Information Packet, Fermilab, January 1998.

[4] T. Trenkler and J.B. Jeanneret, The Principles of Two Stage Betatron and Momentum Collimatin in Circular Accelerators, CERN SL/95-03 (AP), LHC Note 312.

[5] A.A. Sery. ??????????, Workshop on VLHC, Fontana, Wisconsin, February 22-25, 1999.

[6] M. Sidel, Determination of Diffusion Rates in the Proton Beam Halo of HERA, DESY-HERA 93-04 (1993).

[7] J.M. Butler, D.S. Denisov, H.T. Diehl, A.I. Drozhdin, N.V. Mokhov, D.R. Wood, Reduction of TEVATRON and Main Ring Induced Backgrounds in the DØ Detector, Fermilab-FN-629 (1995).

[8] The Large Hadron Collider, Conceptual Design, CERN/AC/95-05(LHC) October 20, 1995.

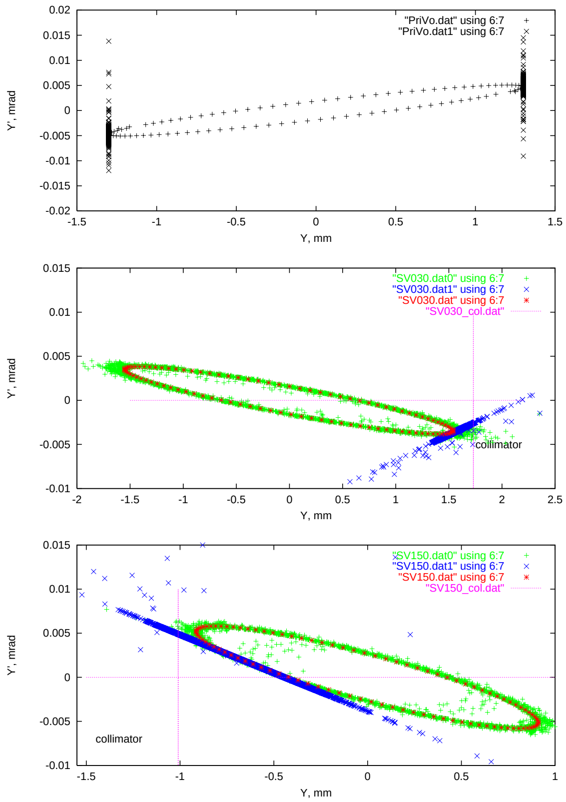

Figure 8: Vertical halo population at the primary PriV collimator exit (top), in the secondary collimator SV030 (middle), and in the secondary collimator SV150 (bottom).

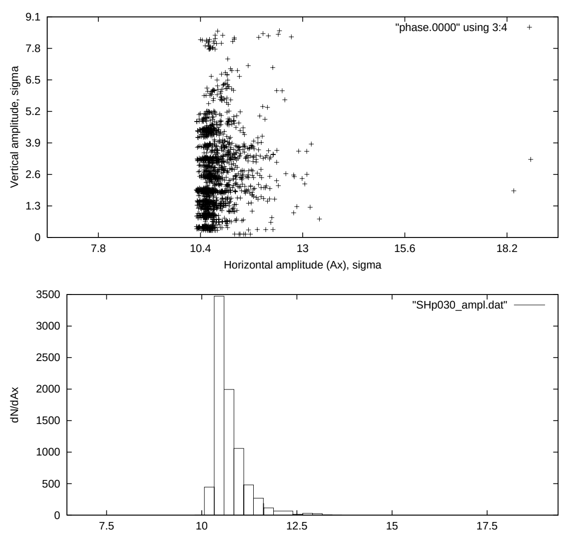

Figure 9: Halo particles population and amplitude distribution in the VLHC aperture at collimation of protons with equilibrium momentum.

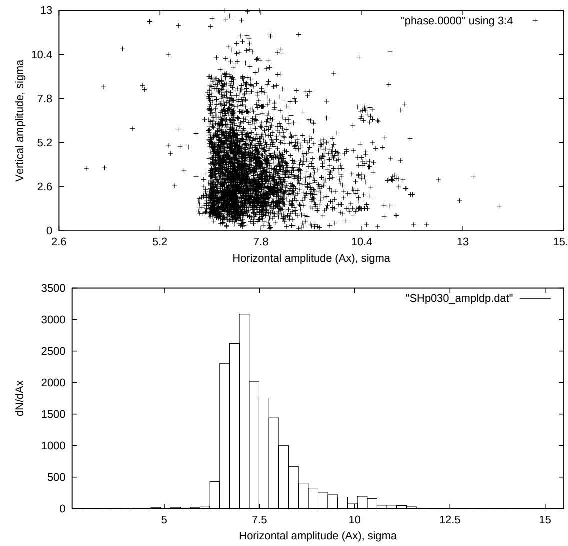

Figure 10: Halo particles population and amplitude distribution in the VLHC aperture at collimation of off-momentum protons with $dP/P = \pm 0.0001$.

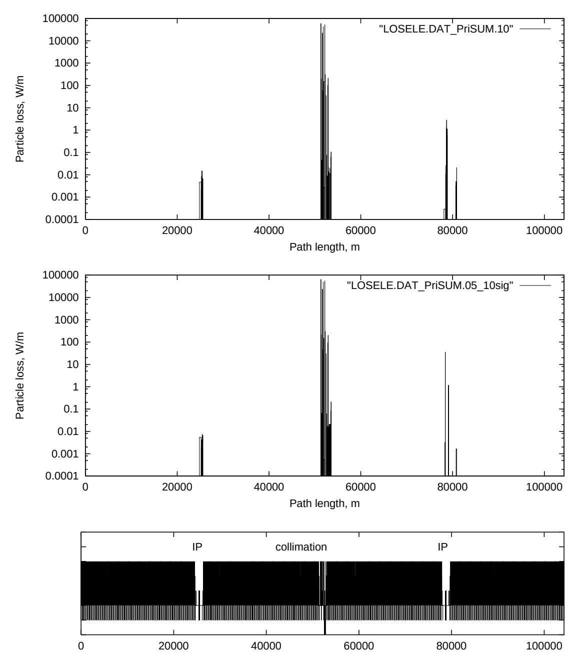

Figure 11: Beam loss distribution along the accelerator at beam collimation with primary collimators at 10σ and secondary collimators at 12σ (top), and with primary collimators at 5σ, secondary collimators at 6.2σ and supplementary collimators at 10σ (bottom).

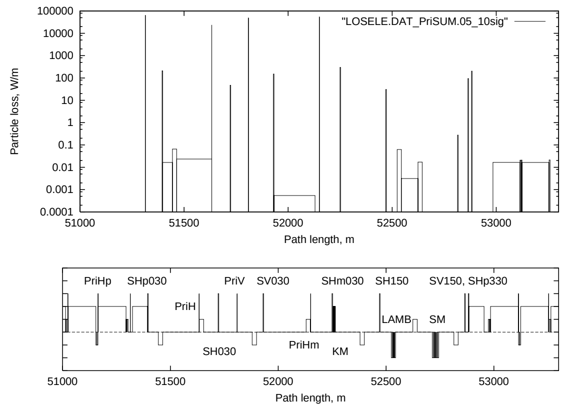

Figure 12: Beam loss distributions in the utility section at beam collimation with primary collimators at 5σ and secondary collimators at 6.2σ.

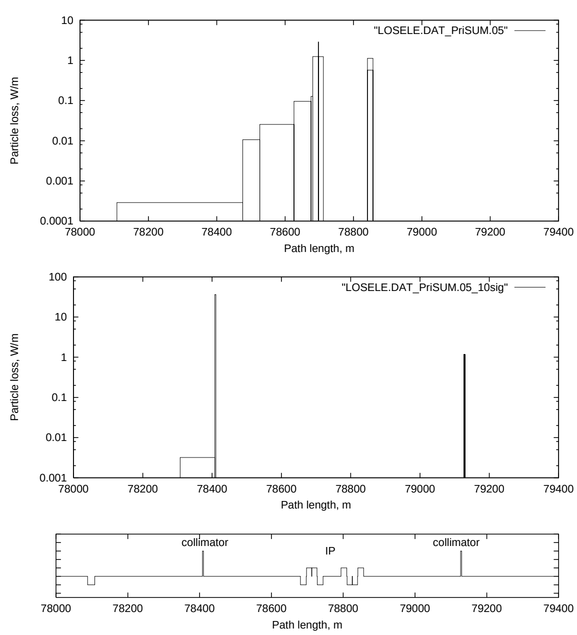

Figure 13: Beam loss distributions in the IR at proton beam collimation without (top) and with supplementary collimators in IR at 10σ (bottom).